

Continental degassing of ^4He by surficial discharge of deep groundwater

Pradeep K. Aggarwal, Takuya Matsumoto, Neil C. Sturchio, Hung K. Chang, Didier Gastmans, Luis J. Araguas-Araguas, Wei Jiang, Zheng-Tian Lu, Peter Mueller, Reika Yokochi, Roland Purtschert, Thomas Torgersen

Hydrogeological setting of Guarani Aquifer

The Guarani Aquifer System (GAS) consists of sandstone layers of Triassic and Jurassic age, deposited in continental and transitional environments, related to important deposits of eolian-fluvio-lacustrine origin, which are classified into two major units: the lower Pirambóia Formation and the upper Botucatu Formation, with a combined average thickness of about 400 m^{1-4} . The aquifer units crop out along narrow bands with a width of about 10-30 km in the western and eastern boundaries of the GAS (Fig. S1) and are confined by basaltic layers of Cretaceous age, reaching, in some places, a thickness of more than 1500 m. Three main hydrogeological domains have been differentiated based on the presence of two major geological structures controlling groundwater flow. The Ponta Grossa Arch and the Asunción-Río Grande Arch (NE-SW) allow the distinction of three major sectors within the GAS.

The aquifer units show important lateral differences in thickness (from less than 50 to more than 700 m, with a mean thickness of about 400 m); they are affected by a number of faults and crossed by volcanic dikes. Despite all these factors, hydraulic continuity of groundwater flow occurs along defined flowpaths. Average aquifer porosity is about 20%. Average hydraulic conductivity and transmissivity are about 2 m d^{-1} and $300\text{ m}^2\text{ d}^{-1}$, respectively, with higher values generally in the upper portion of the aquifer.

The hydrogeological setting of GAS shows evidence of active recharge in the outcrop areas, which are generally located at higher elevations. The potentiometric map in Fig. S1 delineates various flow lines from the highlands in Brazil towards the Paraná River in the northern sector of GAS, and, towards the south or to west (towards some large wetlands in Argentina) in the central and southern sectors. Some of the outcrop areas may function as recharge areas of local shallow groundwater flows and, at the same time, recharge or discharge areas of the deep confined aquifer, especially in the southern border of GAS. While groundwater in the outcrop area is phreatic, highly confined conditions prevail along the major part of the cross section. Groundwaters in the central sector are often artesian, pumped for urban water supply from wells with depths above 1000 m, of good quality and with temperatures ranging from 35 to 55°C.

References:

1. Araújo, L. M. França, B. & Potter, P.E. Hydrogeology of the Mercosul aquifer system in the Paraná and Chaco-Paraná Basins, South America, and comparison with the Navajo-Nugget aquifer system, USA. *Hydrogeol. J.* **7**, 317-336 (1999).
2. Gilboa, Y., Mero, F & Mariano, I.R. The Botucatu aquifer of South America, model of an untapped continental aquifer. *J. Hydrol.* **29**, 165-179 (1976)
3. Consorcio Guarani (2008): Mapa hidrogeológico do SAG. Project for Environmental Protection and Sustainable Development of the Guarani Aquifer System.
4. Organization of American States (2009), Guarani Aquifer: Strategic Action Program – Report on the Project for Environmental Protection and Sustainable Development of the Guarani Aquifer System.

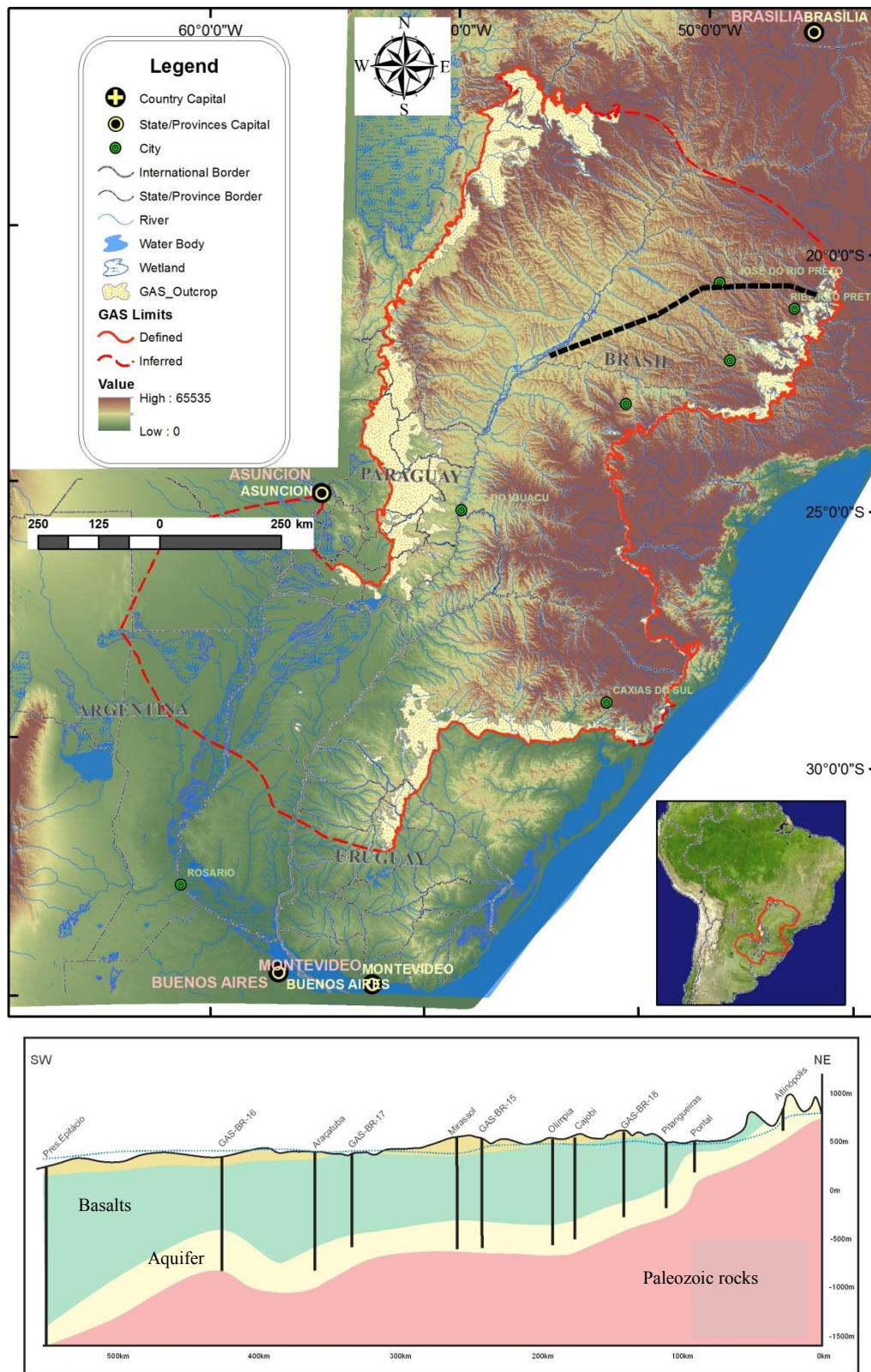


Fig. S1. Spatial extent and relief map of the Guarani aquifer, and a simplified cross section along a southwest- northeast transect (dashed black line) in the northern sector where groundwater samples were collected for this study.

Figure S2. $^3\text{He}/^4\text{He}$ ratios versus Ne/He . The solid line is the least square fits on all data, extending from the crustal $^3\text{He}/^4\text{He}$ ratio to the atmospheric ratio for helium equilibrated with water at 20 °C.

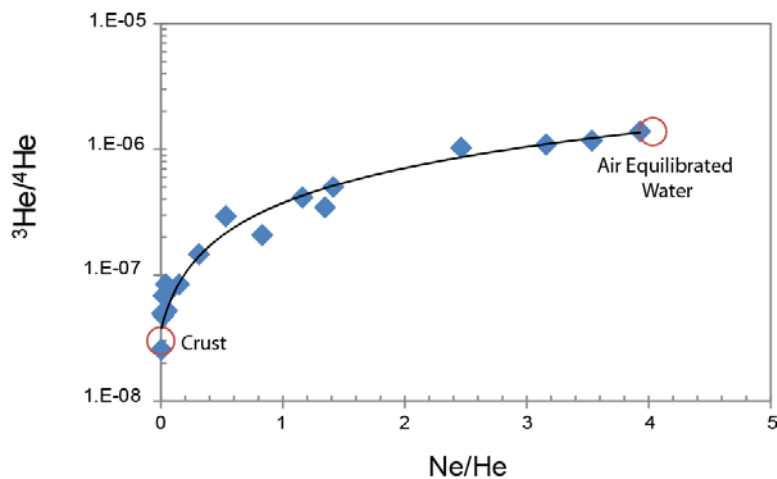


Figure S3. Chloride or Sodium versus $^{81}\text{Kr}/\text{Kr}$ and crustal ^4He . The solid lines either connect or are linear fits for the highest Cl^- or Na^+ concentrations, and are interpreted as mixing lines between the Guarani water and the stagnant water in underlying Paleozoic rocks with $^{81}\text{Kr}/\text{Kr} = 0$ (age > 1 Ma) and Na^+ content of 630 ppm. This constrains the concentration of the crustal ^4He in the end member component to be about $10^{-4} \text{ cm}^3_{\text{STP}} \text{ g}^{-1}$.

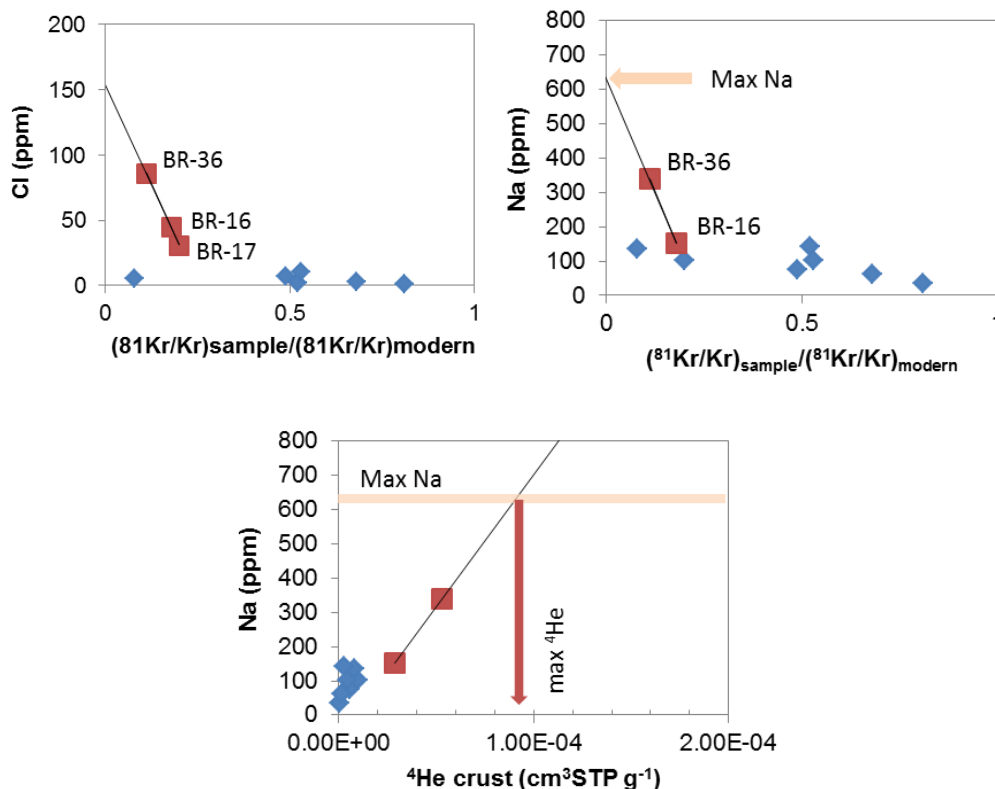


Table ST1. Chemical Composition of Sandstone and Shale from the Guarani Aquifer* and calculated $^3\text{He}/^4\text{He}$ ratios of radiogenic 4He .

Location Lithology ID	<i>Within the Aquifer</i>		<i>Below the Aquifer</i>	
	Sandstone		Sandstone	Shale
	PIR-1	IT-1	COR-1b	
(wt%)				
Al ₂ O ₃	3.1	9.54	9.59	
CaO	0.09	0.01	7.99	
K ₂ O	0.47	3.49	1.19	
Fe ₂ O ₃	1.39	1.91	1.88	
MgO	0.26	0.32	0.92	
MnO	0.01	0.022	0.077	
Na ₂ O	0.079	0.056	2.15	
P ₂ O ₅	0.008	0.057	0.14	
TiO ₂	0.11	0.61	0.36	
SiO ₂	94	83	75	
(ppm)				
Li	4.3	8.7	18	
U	0.6	3.9	2	
Th	1.7	2.2	11	
$^3\text{He}/^4\text{He}$ calc#	9.52E-10	1.87E-09	5.04E-09	

*) Samples are from Rio Claro area in the Guarani. Major element compositions were determined by inductively coupled plasma (ICP)-optical emission spectrometry and Li, U and Th contents were by ICP-mass spectrometry at UNESP, Rio Claro, Brazil.

#) Production ratios of helium isotopes were calculated following the methodology in Mamyrin and Tolstikhin (1984) and Ballentine et al. (2002). Sum of neutron capture probabilities for elements in rock matrices were calculated by using the elemental compositions in this table and average boron concentration of 100 ppm for Palaeozoic sedimentary rocks (Romer and Meixner, 2014).

References

- Ballentine, C. J., Burgess, R., & Marty, B. Tracing fluid origin, transport and interaction in the crust. *Rev. Mineral. Geochem.* **47**, 539-614 (2002).
- Mamyrin, B. A. & Tolstikhin, I. N. *Helium Isotopes in Nature* (Elsevier, Amsterdam, 1984).
- Romer, R. L., & Meixner, A. Lithium and boron isotopic fractionation in sedimentary rocks during metamorphism – The role of rock composition and protolith mineralogy. *Geochim. Cosmochim. Acta*, **128**, 157-177 (2014).